On the Low Temperature Performance of Nickel-Metal Hydride (NiMH) Batteries

Boguslaw Pierozynski

Department of Chemistry, Faculty of Environmental Management and Agriculture, University of Warmia and Mazury in Olsztyn, Plac Lodzki 4, 10-957 Olsztyn, Poland
E-mail: bogpierozynski@yahoo.ca

Nickel-metal hydride (NiMH) batteries are still major battery systems that are commercially used for hybrid electric vehicle (HEV) applications. This is because they are characterized by long durability, safe operation and significantly lower manufacturing cost, as compared to lithium-ion devices, their major competitor for these applications. However, electrochemical performance of NiMH batteries is strongly dependent on the temperature that they are exposed to. Thus, at temperatures below *ca.* -20 ^{o}C, the capacity of nickel-metal hydride batteries significantly declines (as compared to that recorded at room temperature), primarily due to electrochemical deterioration at their negative (MH) electrodes. This work essentially reports on the electrochemical, low-temperature discharge characteristics of a commercial 6.5 Ah/7.2 V NiMH battery module (used for HEV applications), in comparison to those of advanced, AA size NiMH cells.
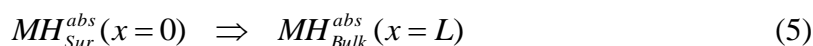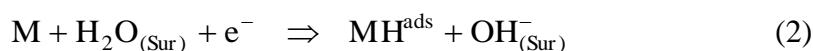
1. INTRODUCTION

Although lithium-ion batteries [1, 2] have occupied the market of small electronic devices (e.g. cell phones, camcorders and portable computers) for many years, advanced nickel-metal hydride (NiMH) batteries are still competitive to Li-ion systems for electric vehicle (EV) and hybrid electric vehicle (HEV) applications. This is because NiMH batteries, in addition to their high-power and long-term durability characteristics could also offer outstandingly reliable and safe operation, and relatively low cost, as compared to the lithium-ion devices [3-11].

Hybrid electric vehicles combine an internal combustion engine (ICE) with an electric motor in the hybrid drive train [4-6], which in addition to improvement of fuel efficiency, leads to significant reduction of car engine emissions. The HEVs are typically powered by high voltage NiMH battery

stacks, which consist of numerous single battery modules connected in series. These modules are stacked side by side and compressed together in a rigid structure, which prevents their expansion from internally-generated pressures. Such battery packs should be able to immediately provide high power to the vehicle's wheels, irrespectively of road and weather conditions. However, it is well-known that nickel-metal hydride batteries could suffer substantial deterioration of electrochemical performance at temperatures below *ca*. -20 ^{o}C (winter conditions) [4, 6, 9, 10, 12, 13].

The rechargeable nickel-metal hydride battery has a similar design to that of nickel cadmium system (NiCd). The principal difference is that the former uses hydrogen absorbed in a metal alloy for the active negative material in place of cadmium in the latter design. The active material of the positive electrode of the NiMH battery is nickel oxy-hydroxide (NiOOH), in the charged state. The negative active material in the charged state is hydrogen, in the form of a metal hydride. During the <u>charging</u> process (discharge proceeds in a reversed sequence of reactions), this metal alloy undergoes a reversible H absorbing-desorbing reaction, as in a sequence of reaction steps (1-5) below:

$$H_2O_{(Bulk)} \quad \Rightarrow \quad H_2O_{(Surf)} \tag{1}$$

$$M + H_2O_{(Sur)} + e^- \quad \Rightarrow \quad MH^{ads} + OH^-_{(Sur)} \tag{2}$$

$$OH^-_{(Sur)} \quad \Rightarrow \quad OH^-_{(Bulk)} \tag{3}$$

$$MH^{ads} \quad \Rightarrow \quad MH^{abs}_{Sur} \,(x=0) \tag{4}$$

$$MH^{abs}_{Sur}(x=0) \quad \Rightarrow \quad MH^{abs}_{Bulk}(x=L) \tag{5}$$

As previously pointed-out in numerous MH electrode and NiMH battery works [12-22], the performance of a metal-hydride electrode is determined by two major factors: the diffusion of absorbed H from the bulk to the electrode surface (reversed step 5) and the kinetics of the charge-transfer reaction (reversed step 2 above). Some role may also be played by the H transfer from the absorbed to adsorbed state (reversed step 4). The electrode discharge capacity will then strongly depend on the rate of its discharge. Diffusion of H and the process of electron transfer are temperature-dependent. Thus, at low temperatures (e.g. below -20 ^{o}C), the performance of MH electrode may significantly decline, leading to reduction of its original capacity at corresponding rates, at room temperature. Moreover, at low temperatures, there are other important factors to be considered, such as changes in the solution conductivity/ionic and molecular mobilities, local ionic concentration gradients built during the dis(charge) process within the porous structure, etc. All these factors may significantly contribute to the performance of the NiMH battery at low temperatures.

This work primarily describes the low-temperature performance of a prismatic, 6.5 Ah (7.2 V) NiMH battery module, which is used for HEV applications (see Fig. 1 below). Its performance is compared with that of the three advanced AA size NiMH cells.
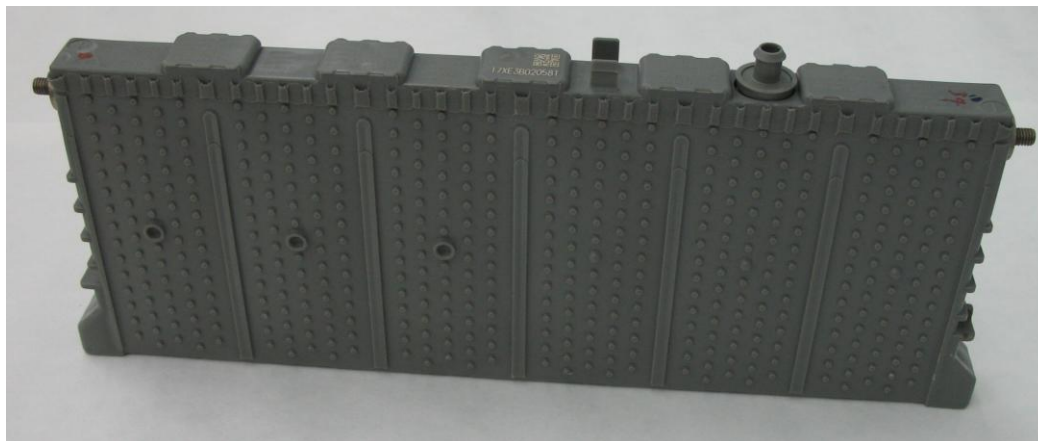
Figure 1. A 6.5 Ah (7.2 V) NiMH prismatic battery module for HEV applications.

2. EXPERIMENTAL

Initially, both the commercial 6.5 Ah NiMH prismatic battery module from Panasonic (consisting of 6 single NiMH cells), as well as the three selected, advanced AA size NiMH batteries [with nominal capacities of 2,000 (Energizer), 2,450 (GP) and 2,650 mAh (Duracell)] were subjected to the cell formation treatments (charge-discharge cycling) at room temperature, realized at 0.1 C (with 40 % overcharge) and 0.2 C (discharge with a cut-off voltage of 0.5 V per single NiMH cell) for the AA cells, and 0.15 C (for charge/discharge with 20 % overcharge) for the 6.5 Ah NiMH battery module. All examined batteries managed to attain their rated capacity values within 5 charge-discharge cycles.

All measurements we conducted by means of the *Solartron* 12608W Full Electrochemical System, consisting of 1260 frequency response analyzer (FRA) and 1287 electrochemical interface (EI). For low temperature experiments (carried-out in a regular Liebherr-brand freezer), battery discharges were conducted for variable C rates, at: -20, -25 and -30 ($\pm$ 1) ^{o}C; while all charges were carried-out at room temperature, at the C rates corresponding to those employed during the cell formation procedures.

3. RESULTS AND DISCUSSION

3.1. Low-temperature performance of the prismatic 6.5 Ah NiMH battery module

The electrochemical discharge characteristics of the prismatic 6.5 Ah NiMH battery module, at various operating temperatures, are shown in Fig. 2 below. It can be observed there that the process of battery discharge at room temperature (carried-out at a slow discharge rate of 0.15 C) leads to the discharge capacity that is almost equal (96 %) to the nominal capacity of this battery module. On the other hand, a dramatic deterioration of the discharge characteristics can be observed when the same

battery module is subjected to very low operational temperatures. Thus, only about 74 and 58 % of the battery nominal capacity could be utilized at -20 and -30 $^{\circ}$C, correspondingly.
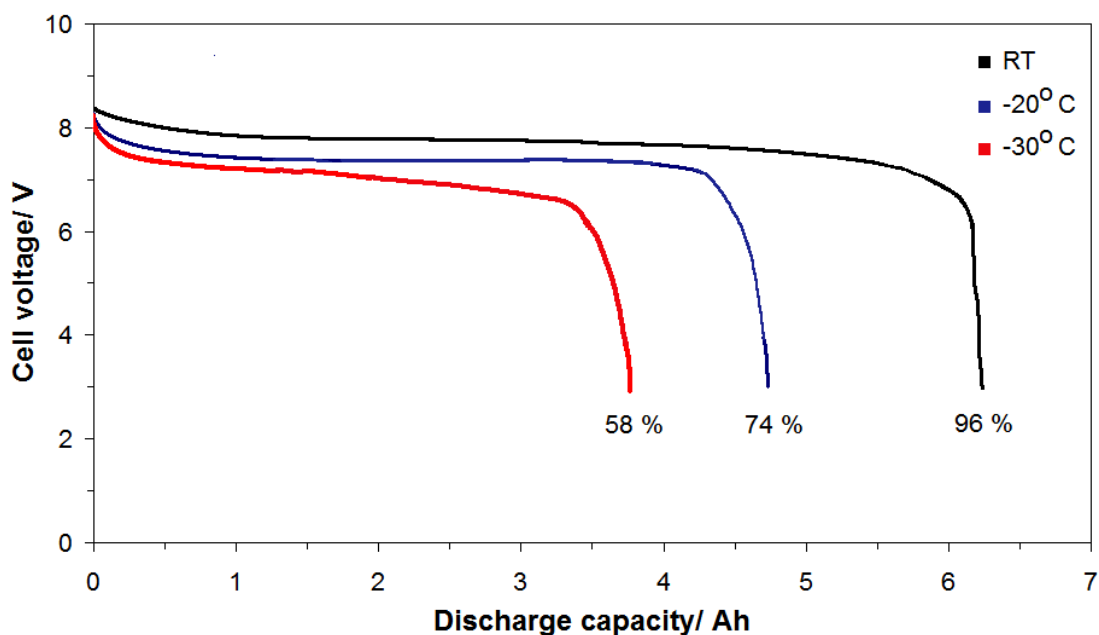

Figure 2. Discharged curves for a 6.5 Ah NiMH prismatic battery module, recorded for a discharge rate of 0.15 C, at: room temperature (RT), -20 and -30 $^{\circ}$C.

In addition, changes of the internal resistance (the sum of reaction components, electrolyte and those resistance elements corresponding to current collectors and inter-connectors) parameter for the battery module were estimated via linear polarization (LP) measurements, carried-out by sweeping the potential (at a scan rate of 0.1 mV s^{-1}) around the rest potential for the selected state-of-charge (SOC) parameter values. Hence, the relative increase (with respect to that recorded at room temperature - RT) of the battery resistance parameter for a fully charged module (100 % SOC) came to *ca*. 3.9 and 5.2, at -25 and -30 $^{\circ}$C, respectively. On the other hand, the respective resistance ratios at 50 % SOC approached 3.1 and 4.8, correspondingly. This dramatic increase of the internal resistance is primarily due to the increase of the reaction resistance [4, 9, 12, 13] at the negative electrodes (anodes), which then has a direct, degrading effect on the battery power characteristics.

3.2.Electrochemical characteristics of advanced AA size battery cells

The discharge performance (carried-out at the discharge rate of 0.5 C) of the three advanced AA size NiMH batteries (Duracell, Energizer and GP), examined at RT and at   -25 $^{\circ}$C, is shown in Fig. 3. Hence, when discharged at room temperature, all batteries almost attained their nominal discharge capacities (94, 96 and 98 % for Duracell, GP and Energizer cells, respectively). It can be observed however in Fig. 3 that the steady discharge voltage for the Energizer cell is *ca*. 200 mV

below those recorded for other tested AA size batteries. Furthermore, for the discharge rate of 0.1 C, the recorded discharge capacities at RT (for the same experimental battery series) were even higher and came to: 96, 99 and 100 % of their nominal capacities.
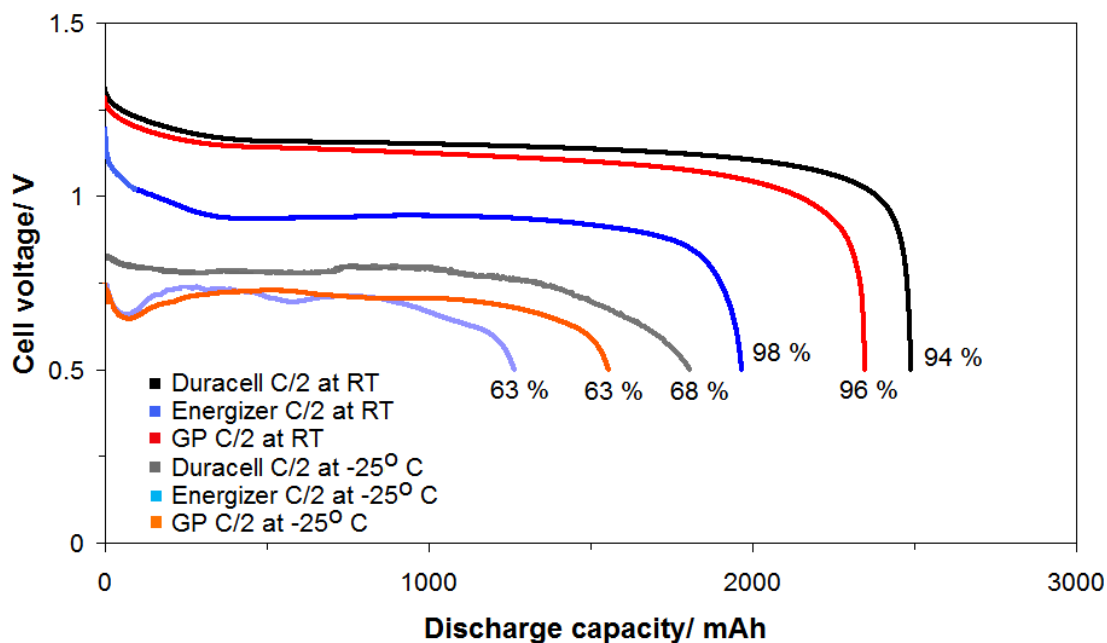
Figure 3. Discharged curves for three advanced AA size NiMH cells (Duracell, Energizer and GP batteries), recorded for a discharge rate of 0.5 C, at: room temperature (RT) and -25 ^{o}C.

Again, a dramatic deterioration of the discharge characteristics can be observed when these batteries are examined at the set temperature of -25 ^{o}C. Thus, for the 0.5 C discharge rate, only about 68 % (for Duracell) and 63 % (for both Energizer and GP cells) of their nominal capacities could be utilized at -25 ^{o}C (the corresponding values for the 0.1 C rate are: 84 % for the Duracell and Energizer cells, and only 70 % for the GP battery). In addition, the fast (0.5 C) discharge process proceeds at considerably diminished cell voltages (by *ca.* 300-400 mV), brought about by substantial electrode polarizations, which occur at this (low) operating temperature. Moreover, the recorded relative increase of the battery resistance parameter (R_{-25}/R_{RT} ratio) for the AA cells is in line with that previously observed for the prismatic 6.5 Ah NiMH battery module. Thus, as an example, the relative increase of the battery internal resistance came for the Energizer cell to *ca.* 3.5 (for 100 % SOC) and 3.9 for 50 % SOC.

4. CONCLUSIONS

Nickel-metal hydride batteries undergo a dramatic deterioration of electrochemical performance at low operating temperatures, specifically for the temperature range below   -20° C. The above is not only evident in case of a large battery module that is used for HEV applications, but also

for advanced AA size battery cells. It is well-known that one of the key reasons for this phenomenon is the kinetics of the charge-transfer reaction (equation 2, reversed step) at the negative (MH) electrode. Numerous attempts have been made to improve the catalytic activity of the MH anode at low temperatures, primarily through introduction of catalytic additives, in the form of ultra-small metallic particles (e.g. Ni, Co, or Cu powders, etc.) to the metal-hydride matrix. The results of some of these works were quite successful on a laboratory scale (see e.g. Refs. 9, 12, 20 and 23).

However, the rate-determining step of the electrode reaction can change from the charge-transfer (equation 2) to the bulk diffusion of H (equation 5, reversed step) or vice versa, in function of the discharge rate and the working temperature parameters. In addition, the battery discharge capability at low temperatures may become significantly affected by lowering of OH^- mobility (equation 3, reversed step), in addition to existence of restricted ionic concentration gradients, possibly leading to local freezing of the water reaction product (equation 1, reversed step) within the porous MH structure.

Therefore, the author of this work suggests another (likely much cheaper) solution to the low-temperature deterioration of electrochemical performance of NiMH batteries, specifically with respect to the HEV applications. It is then suggested that the NiMH battery pack (while on vehicle's board) be enclosed with a special heating mantle, which would also thermally insulate the battery pack from its environment. This low power and electronically-controlled device would then start heating-up the battery pack, whenever ambient temperature dropped below the pre-set temperature value. Also, the battery package could be heated-up (in a controlled manner) to e.g. 0 ^{o}C, but only prior to the planned car driving. It is strongly believed that the above-mentioned procedure would significantly help preserve the high-power performance of the NiMH battery package at ambient temperatures as low as -30 ^{o}C.

References

1. B. Scrosati, J. Garche, *J. Power Sources*, 195, (2010), 2419.
2. A.Ritchie, W. Howard, *J. Power Sources*, 162, (2006), 809.
3. M.L. Soria, J. Chacon, J.C. Hernandez, *J. Power Sources*, 102, (2001), 97.
4. A.Taniguchi, N. Fujioka, M. Ikoma, A. Ohta, *J. Power Sources*, 100, (2001), 117.
5. D.W. Corson, *J. Power Sources*, 105, (2002), 110.
6. O. Bitsche, G. Gutmann, *J. Power Sources*, 127, (2004), 8.
7. T. Tanaka, M. Kuzuhara, M. Watada, M. Oshitani, *J. Alloys Comp.*, 408-412, (2006), 323.
8. W.K. Hu, M.M. Geng, X.P. Gao, T. Burchardt, Z.X. Gong, D. Noreus, N.K. Nakstad , *J. Power Sources*, 159, (2006), 1478.
9. M.A. Fetcenko, S.R. Ovshinsky, B. Reichman, K. Young, C. Fierro, J. Koch, A. Zallen, W. Mays, T. Ouchi, *J. Power Sources*, 165, (2007), 544.
10. S. Shi, C. Ouyang, M. Lei, *J. Power Sources*, 164, (2007), 911.
11. X. Zhang, Z. Gong, S. Zhao, M. Geng, Y. Wang, D.O. Northwood, *J. Power Sources*, 175, (2008), 630.
12. H. Ye, H. Zhang, *J. Electrochem. Soc.*, 149(2), (2002), A122.
13. Y. Liu, H. Pan, M. Gao, Y. Zhu, Y. Lei, Q. Wang, *Electrochim. Acta*, 49, (2004), 545.
14. N. Kuriyama, T. Sakai, H. Miyamura, I. Uchara, H. Ishikawa, T. Iwasaki, *J. Alloys Comp.*, 202, (1993), 183.
15. L.O. Valoen, A. Lasia, R. Tunold, *Electrochem. Soc. Proc.*, 16, (2000), 133.

16. B. Reichman, W.C. Mays, K. Young, M.A. Fetcenko, S.R. Ovshinsky, *Electrochem. Soc. Proc.*, 15, (1998), 111.
17. M. Geng, F. Feng, P.J. Sebastian, A.J. Matchett, D.O. Northwood, *Int. J. Hydrogen Energy*, 26, (2000), 165.
18. C. Wang, M.P. Soriaga, S. Srinivasan, *J. Power Sources*, 85, (2000), 212.
19. X. Yuan, N. Xu, *J. Alloys Comp.*, 316, (2001), 113.
20. A.Yuan, N. Xu, *J. Alloys Comp.*, 322, (2001), 269.
21. X. Yuan, N. Xu, *J. Electrochem. Soc.*, 149(4), (2002), A407.
22. M. Mohamedi, T. Sato, T. Itoh, M. Umeda, I. Uchida, *J. Electrochem. Soc*., 149(8), (2002), A983.
23. F. Feng, D.O. Northwood, *Surf. Coat. Technol*., 167, (2003), 263.